

Multiple ionization, fragmentation and dehydrogenation of coronene in collision with swift proton

Shashank Singh,¹ Sanjeev Kumar Maurya,¹ Laszlo Gulyás,² and Lokesh Tribedi^{1,*}

¹*Department of Nuclear and Atomic Physics, Tata Institute of Fundamental Research,
Dr. Homi Bhabha Road, Colaba, Mumbai 400005, India*

²*Institute of Nuclear Research of the Hungarian Academy of Sciences (ATOMKI), H-4001 Debrecen, Hungary
(Dated: January 7, 2025)*

The coronene molecules have been bombarded by protons of energy by 75-300 keV. The time of flight mass spectrum has been recorded using a two-stage Wiley-McLaren type spectrometer. A large enhancement in the doubly and triply ionized recoil ion is observed compared to the singly ionized one. The single, double and triple ionization yields have also been calculated using the continuum distorted wave-eikonal initial state (CDW-EIS) theoretical model and are compared with the experimental results. Experimental double-to-single ionization yield ratios and triple-to-single ionization yield ratios have been compared with the theoretical ratios which are found to be much higher w.r. t. the gas atoms. Evaporation peaks due to the loss of several neutral C_2H_2 and C_3H_3 are observed corresponding to their parent singly, doubly and triply charge coronene ions. Small fragmentation peaks $C_nH_x^+$ ($n = 3-7$) are present in the spectra due to higher energy transfer by the projectile to the molecule. The hydrogen losses are observed in the cation, di-cation and tri-cation coronene peak structures. A maximum of the 7 H-losses are detected which depends on the beam energy.

INTRODUCTION

Polycyclic aromatic hydrocarbon (PAH) molecules are widely observed in diffuse interstellar bands (DIBs) via the absorption spectra in the optical region (0.4 and 1.3 μm)[1–3] and in aromatic infrared bands (AIBs) via the infrared emission spectra [1, 4]. The DIBs are discovered in the line of sight of stars through various interstellar objects and in the extra-galactic environment. The AIB of the interstellar objects appears due to the presence of highly vibrationally excited PAHs which are induced by the ultraviolet-visible and near-infrared radiation [5]. The PAHs are also possible carriers of the extended red emission (ERE: 540 nm to 900 nm) [6–8]. Using the quantum chemistry calculations, Rhee et al. predicted that the possible carriers of the ERE are the PAH dimers ($[PAH_2]^+$) [8]. Moreels et al. proposed the PAHs are the carriers of the unknown fluorescence bands which were detected in the 280 to 480 nm range by the three-channel spectrometer (TKS) onboard the Vega 2 spacecraft in the coma of comet Halley [9]. Allamandola et al. modeled the infrared band spectrum of various interstellar objects using laboratory spectra of neutral and ionized PAHs [10]. The PAHs are present in the galaxy and extragalactic sources, outer solar system bodies, local interstellar and other galaxies, reflection nebulae planetary nebulae, meteorites, interplanetary dust particles and interstellar objects.

The PAH molecules are composed of two or more aromatic rings and get stabilized by the delocalization of the pi electrons. These molecules are reported and stabilized by the delocalization of the electrons. The ionization potential and the dissociation energies of the PAHs molecules (a few tens of eV [11]) are high due to

which they survive in the harsh interstellar environment by the exposure of UV and heavy ions [12, 13]. The ionization state of the PAHs gives information about the ionization balance of the medium, while the size and composition give the energetic and chemical history of the medium. Allamandola et al., Leger and Puget proposed a model to identify the presence of PAHs in the interstellar medium [4, 14].

Earlier, few PAHs have been used for photon, electron, proton and heavy ions-induced ionization and fragmentation studies. Lawicki et al. studied the multiple ionization and fragmentation of coronene ($C_{24}H_{12}$) and pyrene ($C_{16}H_{10}$) molecules by the impact of He^{2+} , O^{3+} and Xe^{20+} ions at low velocity ($v \leq 0.6$ a.u.) [15]. Bagdia et al. reported the ionization and fragmentation of fluorine molecules bombarded by the 250 keV protons and found a substantially large doubly to singly charged production ratio in comparison to the He and Ne targets [16]. Chen et al. studied the formation of molecular ions by the impact of He^+ ions on the anthracene ($C_{14}H_{10}$), pyrene and coronene molecules [17]. The hydrogen loss signature has been observed in the single, doubly and triply ionized coronene peak which is important to understand the formation of hydrogen molecules in interstellar medium. Holm et al. studied the collisions of 11.25 keV $^3He^+$ and 360 keV $^{129}Xe^{20+}$ ions with the weakly bound clusters of anthracene ($C_{14}H_{10}$) and found that the $C_{14}H_{10}$ clusters have higher tendencies to fragment in ion collisions than other weakly bound clusters [13]. Chen et al. presented a scaling law for the absolute cross sections for non-statistical fragmentation in collisions between PAH/PAH^+ and hydrogen or helium atoms with kinetic energies ranging from 50 eV to 10 keV [18].

Hydrogen is the most abundant atom in the interstellar medium. It is known that the abundance of H_2 in the cold interstellar medium can not be explained by only considering the reactions in the gas phase [19]. Association of H on the surface of interstellar dust grain [20, 21] is one possible way to form molecular hydrogen in the interstellar medium. In another possible way, interstellar Polycyclic aromatic hydrocarbon (PAHs) act as catalysts in hydrogenation reaction [22–24]. Also, it has been reported that the interaction of various ionizing radiation to PAHs can be one of the possible causes of the H_2 formation via the dehydrogenation process in the interstellar medium. Champeaux et al. reported the H-loss in the coronene molecule by the impact of 100 keV protons and observed one H_2 and two H_2 losses in cation, dication and trication [25]. They suggested that along with the CH_2 precursor, energetically, the formation of the H_2 is more favorable than $2H$. Also, Giard et al. reported the first results obtained on the photo-dissociation of the isolated PAH cations, such as, $^{12}C_{24}H_{12}^+$, $^{13}C_1^{12}C_{23}H_{12}^+$ and $^{12}C_{24}H_{10}^+$ [26]. Joblin et al. suggested that the PAHs may be the major catalysts in the formation of molecular hydrogen in the ISM [27].

In this sequence, in the present experiment, we have studied the interaction of the low-energy protons with the gas phase coronene molecule. This study is important to understand the ionization and fragmentation mechanism of large PAHs by the energetic heavy ions. The experiment resembles the collision of heavy ions in space making this study more interesting. The details are discussed below.

EXPERIMENTAL DETAILS

The experiment was performed at the Electron Cyclotron Resonance Ion Accelerator (ECRIA) facility situated at TIFR, Mumbai (India) [28, 29]. Protons of energy 100–300 keV have been extracted from the machine to bombard the coronene molecules. The beam was collimated by the two sets of 4-jaw slits situated at a distance of 37.8 cm from each other at the beamline and a 2 mm diameter stainless steel collimator placed before the chamber. An oven used to heat the coronene which was placed in the center of the chamber and below the interaction region. A nozzle of the aspect ratio 10 and an opening of 1 mm was used to produce the effusive jet. The temperature of the molecule was controlled by the two variacs. These variacs were connected in series through a step-down transformer in to control the temperature in fine steps. The commercially available powder of the coronene (99.99%) molecule was heated up to 160 °C. The temperature was monitored by a thermocouple attached to the oven. The vapor density of the coronene molecule could be increased by the increasing tempera-

ture. A gold crystal in a crystal holder was placed just above the interaction region to measure the thickness of the deposited coronene. This crystal was connected to the INFICON SQM-160 thickness monitor placed above the oven was used to monitor the rate of vapor flow.

The two-stage Wiley-McLaren type spectrometer was used with a slight modification by employing a lens [30] in between the acceleration region and the drift tube. This spectrometer was placed in the chamber perpendicular to the beam direction. The details of the spectrometer were published by Biswas and Tribedi [30]. However, a brief detail is also given here. The TOF spectrometer is divided into three regions namely, the extraction (E), acceleration (A) and drift region (D). The extraction region has two electrodes, a pusher and a puller. There are four electrodes in the acceleration region which are connected by 10 MΩ resistances. Additionally, a pair of electrodes (lens electrodes) were used in between the acceleration region and drift region to obtain better 4π collection efficiency with larger angular acceptance [30]. A 1.5 mm diameter hole into the pusher plate was used to collimate the generated electrons and to reduce the background. The voltage given to the pusher, puller, accelerator end, lens electrodes and drift tube were +225, -225 volts, -1905, -1515, and -1940 volts, respectively. Ni grid (90 % transmission) was placed at the puller, the accelerating end and at the end of the drift tube to avoid field penetration. At the other end of the spectrometer, a channel electron multiplier (CEM) (20 mm diameter) is placed to detect the recoil ions of coronene and fragmented ions. At the other end, before the pusher, another CEM of diameter 10 mm was placed to detect the ionized electrons. The electron-ion coincidence spectra have been recorded using these CEM. The electron-CEM gives the start signal and ion-CEM gives the stop signal within a selected window of 20 μ s. Typical schematic chamber of the experimental setup is shown in Fig. 1. The vacuum of the chamber was maintained at about 1×10^{-7} torr by using a turbo-molecular pump during the experiment.

RESULTS AND DISCUSSIONS

The typical mass to charge ratio (m/q) calibrated TOF spectra for the coronene molecule bombarded by the 100, 200 and 300 keV protons are shown in Fig. 2. The peaks of cation, di-cation and tri-cation of coronene molecules are observed in the spectra (Fig. 2). Fig. 3 shows the enlarged view of the spectrum (Fig. 2) corresponding to the evaporation and fragmentation peaks of $C_{24}H_{12}^{2+}$ and $C_{24}H_{12}^{3+}$. One evaporation peak $C_{20}H_{12}^+$ of cation by the loss of C_2 is observed Fig. 2. The evaporation peaks of the parent di-cation by the loss of single, double and triple C_2H_2 ($C_{22}H_{10}^{2+}$, $C_{20}H_8^{2+}$ and $C_{18}H_6^{2+}$, respectively) are present in Fig. 3. The evaporation peaks of the tri-cation by the loss of one C_2H_2 ($C_{22}H_{10}^{3+}$) is

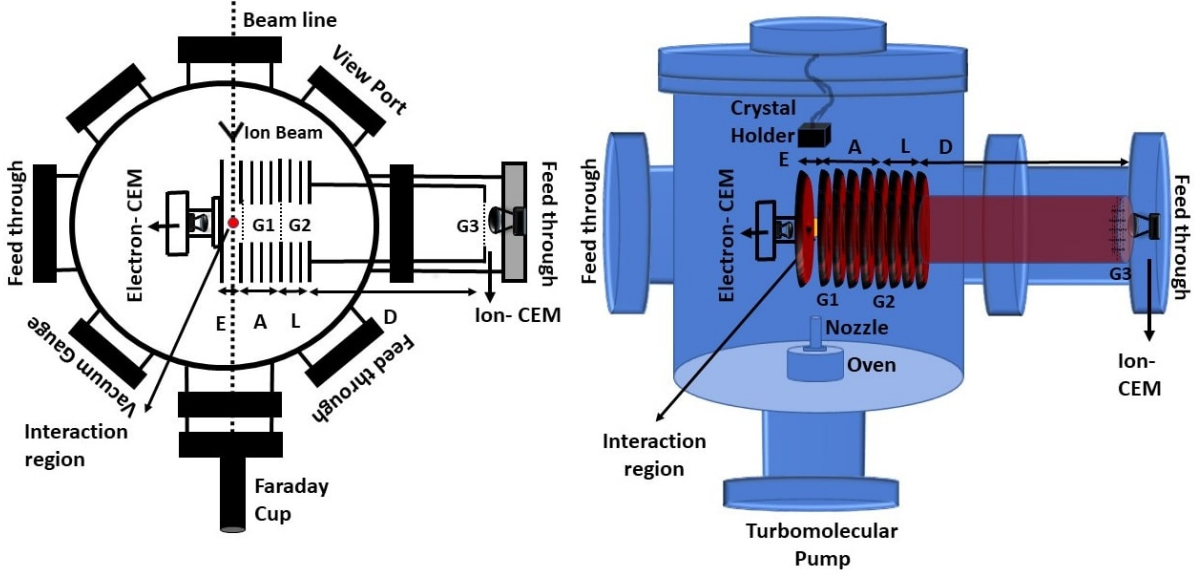


FIG. 1. Typical schematic chamber of the experimental setup (left one: upper view; right one: front view)

present in Fig. 3. The fragmentation product C_nH_x ($n = 3 - 7$) are also present. The peaks of O_2^+ , N_2^+ , H_2O^+ , OH^+ , O^+/O_2^{2+} , N^+/N_2^{2+} are attributed to the background gases. The peak of H^+ appears due to the H^+ losses by the coronene molecules and H_2O molecules (which are present in the coronene powder).

Lawicki et al. observed up to triply charged coronene cation due to the bombardment of He^{2+} and O^{3+} ions with the coronene [15]. They also observed up to $C_{24}H_{12}^{5+}$ intact ions due to the impact of Xe^{20+} ions on coronene. In the present case, we could detect up to tri-cation of coronene because of the lower charge state of proton than the He^{2+} ions. We have observed three evaporation peaks ($C_{22}H_{10}^{2+}$, $C_{20}H_8^{2+}$, $C_{18}H_8^{2+}$) for di-cation and two evaporation peaks ($C_{22}H_{10}^{3+}$, $C_{21}H_{10}^{3+}$) for tri-cation, which are due to greater momentum transfer to the molecule by the projectile. The peak $C_7H_3^+$ is mixed with the peak $C_{21}H_{10}^{3+}$ (C_3H_3 loss). The observed yield of $C_{22}H_{10}^{3+}$ (C_2H_2 loss) is lesser than the $C_7H_3^+$. It shows that the contribution of the C_3H_3 loss should be smaller than the $C_{22}H_{10}^{3+}$ in $C_7H_3^+$ peak because of higher binding energy of C_3H_3 than C_2H_2 . Also, Dyakov et al. studied that the C_3H_3 loss channel is negligible for photodissociation of azulene cation by the ab initio and Rice–Ramsperger–Kassel–Marcus (RRKM) study [31]. So we can assume that for smaller fragmentation peaks (C_nH_x ; $n = 3 - 7$) there is no contribution from C_3H_3 evaporation.

The experimental yields and theoretical cross-sections (CDW-EIS) of coronene cation, di-cation and tri-cation w.r t. the projectile energies are plotted in Fig. 4. The uncertainties in the data are within 13%. The experimental yield values are normalized by the 200 keV theoretical

cross-section. The yields of the singly, doubly and triply coronene ions are normalized for CEM efficiency as per the efficiency plot given in Krems et al. [32]. The efficiency values of the channeltron for singly, doubly and triply charged coronene has been taken as 0.12, 0.29 and 0.44, respectively. For the double and triple ionization, the chance of detecting electrons is double and triple in comparison to the single ionization. Therefore, the yields of the doubly and triply ionized coronene are divided by a factor of 2 and 3, respectively. The experimental yields of cation, di-cation and tri-cation show a similar trend as the theoretical cross-section. In the yield of cation only direct ionization (DI) is present whereas in the di-cation and tri-cation transfer ionization (TI) is also included. Production of di-cations could be due to the combination of 2 DI or 1 DI and 1 TI processes. Similarly, the production of tri-cations could be due to the combination of 3 DI or 2 DI and 1 TI. The transfer ionization cross-section falls more sharply with energy which is reflected in the experimental yield of the di-cation and tri-cation. At the lower projectile energies (75 and 100 keV), the experimental yield of di-cation and tri-cation are higher than the theoretical values due to higher transfer ionization cross-section.

Double-to single and triple-to-single ionization ratio

The energy dependence of the experimental yield and theoretical cross-section ratios are plotted in Fig. 5, which is found to be decreasing. The uncertainty in the data is typically $\approx 17\%$. The yield ratio of doubly (R_{21}) and triply (R_{31}) charged coronene w. r. t. the singly

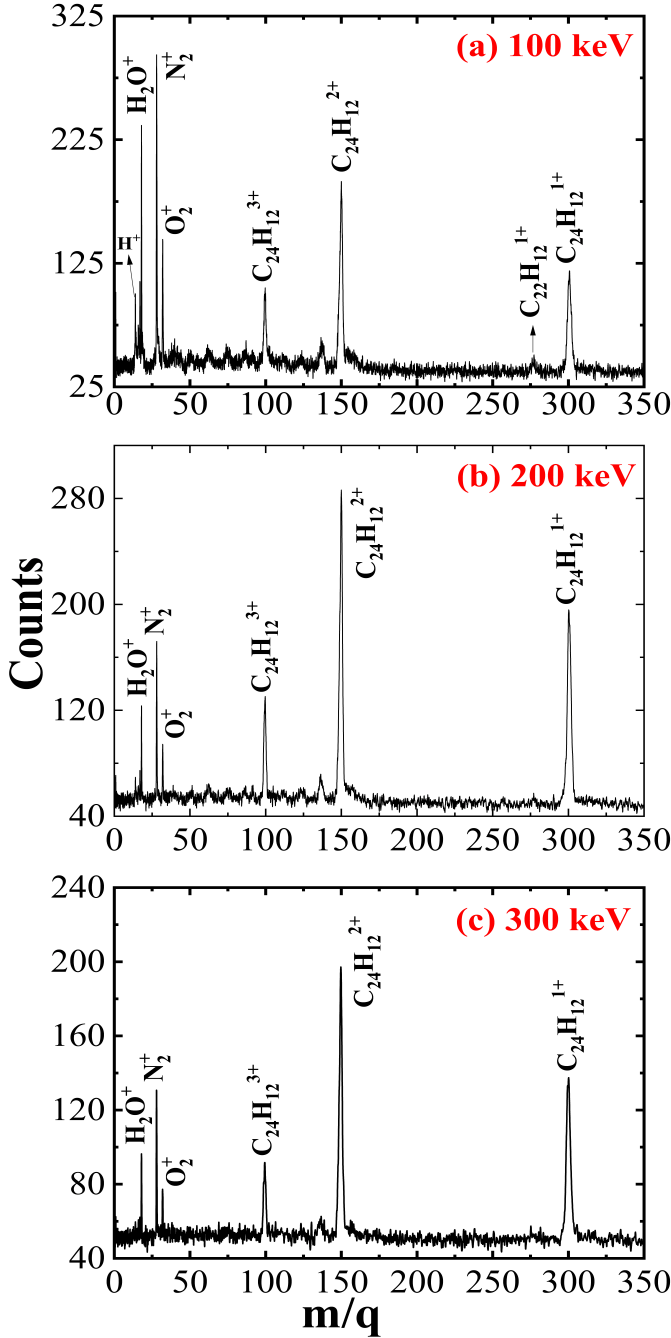


FIG. 2.

(a), (b) and (c) Typical TOF spectrum of coronene as a function of m/q for three different energies, 100, 200 & 300 keV

charged coronene are determined to be 0.47 and 0.12, respectively, at the lowest energy (75 keV). At the highest energy (300 keV), the yield ratios are found to be 0.19 and 0.01, respectively. These ratios R_{21} are substantially large compared to the other gas targets [16]. The ratio R_{21} for Ne and He targets by the impact 250 keV proton is about 0.13 and 0.011, respectively [16]. The experi-

mental R_{21} values are falling sharper than the theoretical values. The experimental R_{31} values are significantly higher than the theoretical values except at higher projectile energies.

The study of double ionization of various targets by the impact of charged particles has been quite interesting for decades [33–40]. In earlier studies, on the He-atom the DI process was explained by two-step 1, two-step 2 and shake-off mechanism. In the present study, higher experimental yield ratios may be due to several reasons. The theoretical limitation is the main reason for disagreement between the theoretical and experimental ratios. CDW-EIS theory is based on independent electron approximation in which one electron is considered active and others are treated like passive electrons. Importantly, multi-electron correlation is not taken care of in the theory. It includes only DI, not TI. The unexpectedly large doubly or triply ionized recoil-ions of the PAH molecules could be related to the highly correlated electron cloud and possible plasmonic states excited during the collisions. Such plasmonic behavior has been reported for coronene and fluorene in heavy ion collisions [41, 42].

Hydrogen loss

The enlarged peak structures of coronene cation, di-cation and tri-cation for 100, 200 and 300 keV projectiles are shown in Fig. 6. The peak structures have been fitted by multi-Gaussian function. The maximum fitting uncertainty for the centroid of the peak is $m/q = 0.4$. The peaks right to the parent cation are attributed to the presence of $^{13}C_1$ and $^{13}C_2$ isotopes in the coronene molecule. The peaks to the left of the di-cation ($m/q = 150$) (i.e. $C_{24}H_{12}^{2+}$, $m/q = 150$) are attributed to the even number of H losses (2, 4 and 6) and the right correspond to $^{13}C_2$ isotope. Similarly, the peak structure around $m/q = 100$ is fitted for several peaks. The peaks left to the tri-cation peak (at $m/q = 100$) are attributed to the 1-6 H losses peaks and to the right correspond to the $^{13}C_1$, $^{13}C_2$ and $^{13}C_3$ isotopes. Similarly, for the 300 keV projectile the fitted singly, doubly and triply ionized coronene ion peaks are shown in Fig. 6. The fitted peak structure for singly and doubly ionized coronene ions at 300 keV are the same as that for 100 keV. But for the triply ionized coronene at 300 keV, there is one additional peak fitted at $m/q = 97.66$ value corresponding to the 7 H losses which was missing for the 100, 200 keV projectile.

There is one extra number of H loss in cation and tri-cation for 300 keV projectile and the yields of the H losses increase w. r. t. the parent ion. The yield of the 1 H, 2 H and 3 H loss in tri-cation are more than the parent ion at 100 keV as the internal energy of the tri-cation is more. The yield of the 1 H loss in the cation, 2 H loss in the di-cation and up to 4 H loss in the tri-cation yields are more than the parent ion at 300 keV projectile energy.

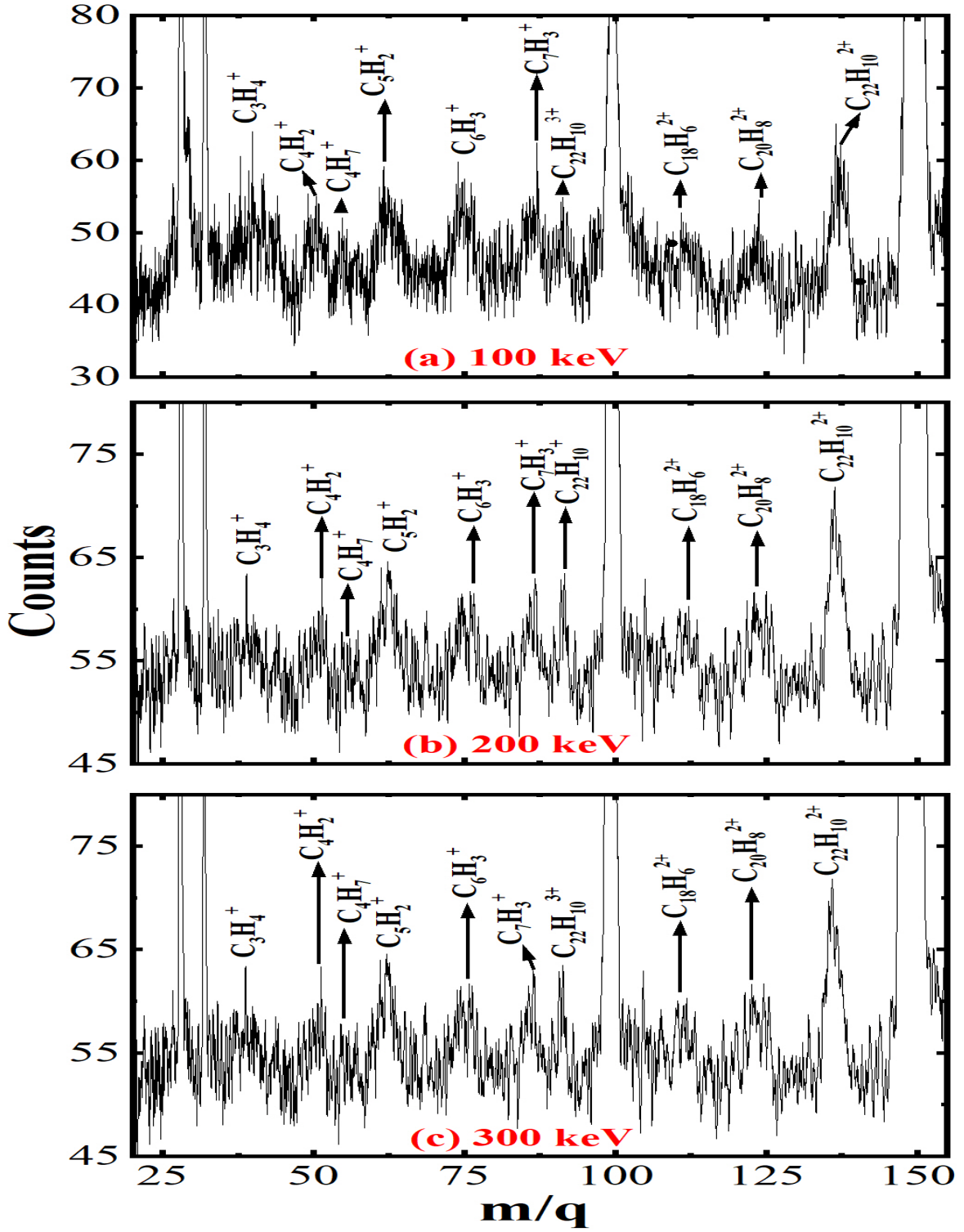


FIG. 3.

(a), (b) and (c) enlarged view of Fig: 2(a), (b) and (c) for evaporation peaks of $C_{24}H_{12}^{2+}$ and $C_{24}H_{12}^{3+}$ (m/q range from 20 to 160) for 100, 200 and 300 keV projectile energy

This is due to the higher internal energy of the coronene molecule imparted by a more energetic projectile. The percentage contribution of parent ion, H losses and ^{13}C

isotopic peaks are tabulated in Table I. It shows for example $C_{24}H_{12}^{2+}$ the parent ion fraction is 45% while the H losses constitute the rest 55% at 100 keV. At higher

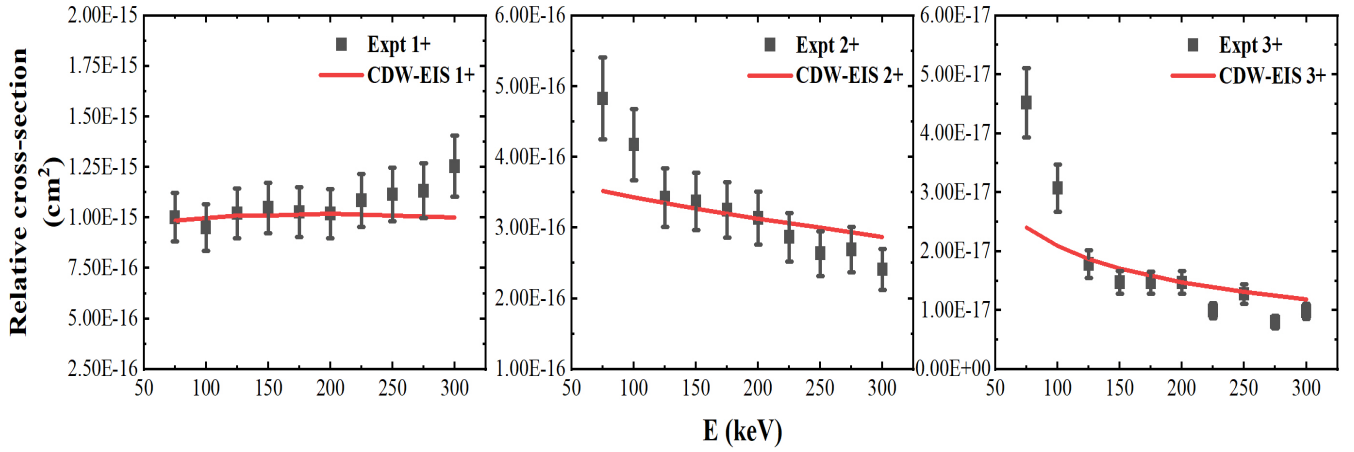


FIG. 4. Experimental yield (black squares) and CDW-EIS theoretical yield (red dots joining with line) of the singly, doubly and triply ionized coronene; the experimental yield is normalized by the theoretical cross-section at 200 keV

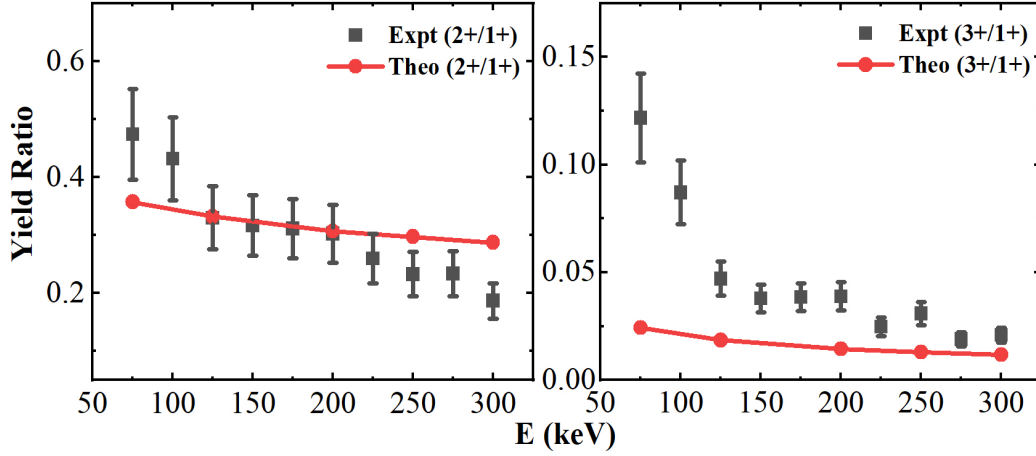


FIG. 5.

Yield ratio of the doubly to singly and triply to singly ionized coronene ion (black points) and the theoretical (CDW-EIS) values (red line with circle)

energy H-loss contribution reduced from 55% to 31% (at 300 keV).

Earlier in similar studies [43–45], various PAH cations had been exposed to the VUV radiation, showing the H loss from the cations. Champeaux et al. observed only an even number of H losses (up to 4 H loss) in the coronene cation, di-cation and tri-cation by the 100 keV proton impact [25]. Because of only even number of H losses were present, they suggested that the elimination of H_2 is energetically more favorable than the 2H along with CH_2 precursor. But, in the present study, we observed both even and odd H losses for cation and tri-cation. Surprisingly, only an even number of H losses are present in di-cation. Lawicki et al. observed no H loss in cation and up to 4 H loss in di-cation (only even) of coronene by the impact of Xe^{20+} [15]. Also, they observed up to 4 H loss in cation (both even and odd) and up to 6 H loss in di-cation (only even) of coronene by the impact of He^{2+}

ions. These results are similar to our result in the aspect of even and odd H losses.

CONCLUSIONS

The time of flight spectrum has been recorded for the coronene molecule by the bombardment of protons using a two-stage Wiley McLaren type spectrometer. We detected up to tri-cation of coronene along with evaporation and fragmentation peaks. The energy dependence of the relative cross section of cation, di-cation and tri-cation show the same pattern as the theoretical model (CDW-EIS) i.e. reducing with energy for 2+ and 3+. A dramatically enhanced 2+/1+ and 3+/1+ ratios are found which are much larger than the typical gaseous targets which could be due to highly correlated electron cloud and the plasmonic excitation (studied earlier). In

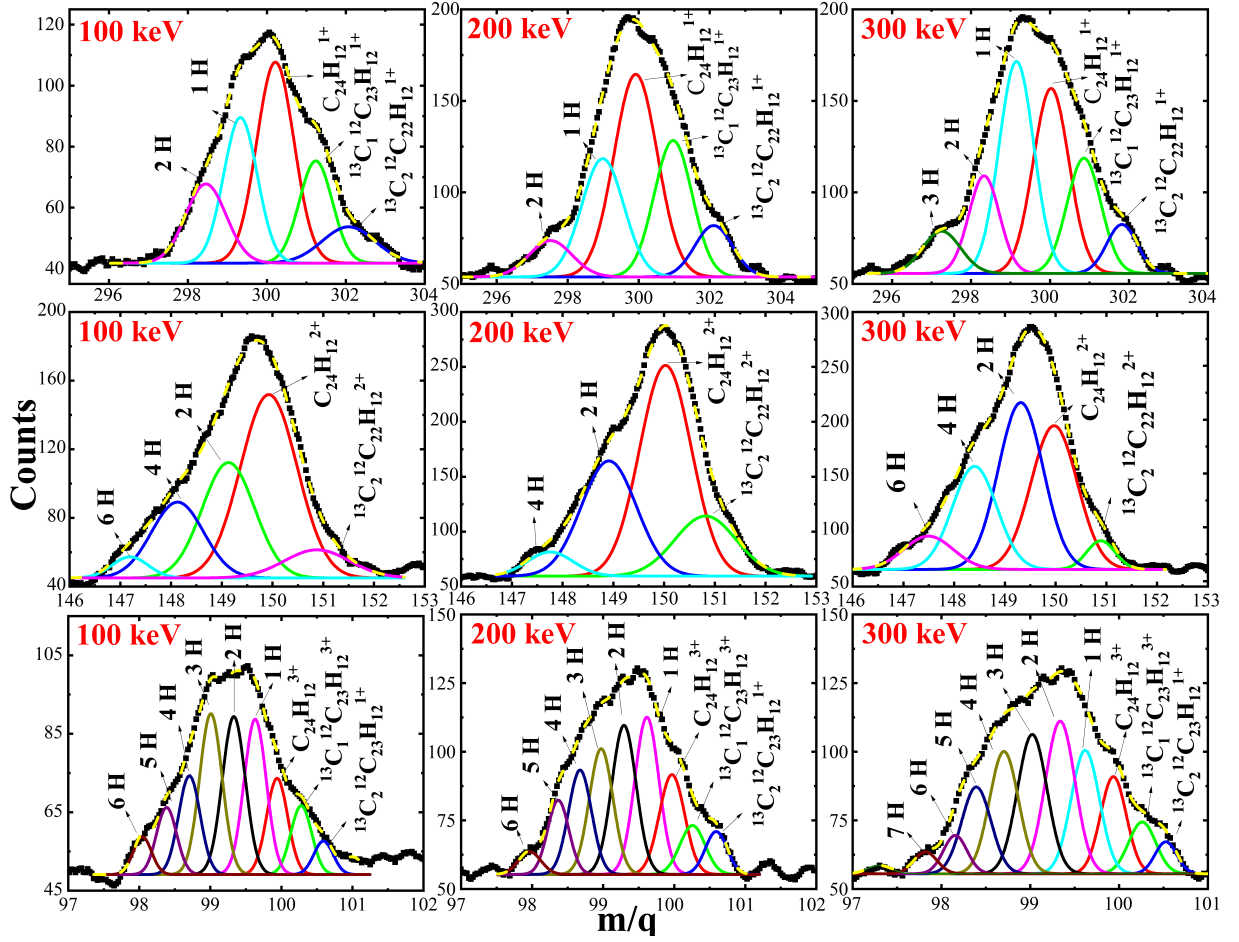


FIG. 6.

Singly, doubly and triply ionized coronene showing H-loss components by multi-Gaussian fitting (black solid curve: observed peak structure, yellow dashed curve: fitted peak structure)

TABLE I. Contribution of the parent, nH losses (n=1 to 8) and carbon isotope in the singly, doubly and triply ionized corenene recoil-ions at 100, 200 and 300 keV projectile

| E (keV) | species/ion | parent ion | 1 H | 2 H | 3 H | 4 H | 5 H | 6 H | 7 H | 8 H | $^{13}\text{C}_1$ | $^{13}\text{C}_2$ | $^{13}\text{C}_3$ |
|---------|-----------------------------------|------------|------|------|------|------|------|-----|-----|-----|-------------------|-------------------|-------------------|
| 100 keV | $\text{C}_{24}\text{H}_{12}^{1+}$ | 31.8 | 25.3 | 13.6 | — | — | — | — | — | — | 24.9 | 4.3 | — |
| | $\text{C}_{24}\text{H}_{12}^{2+}$ | 45.2 | — | 26.2 | — | 17.2 | — | 3.3 | — | — | 8.0 | — | — |
| | $\text{C}_{24}\text{H}_{12}^{3+}$ | 10.4 | 17.8 | 18.8 | 18.7 | 11.0 | 6.9 | 3.6 | — | — | 7.4 | 3.3 | 1.8 |
| 200 keV | $\text{C}_{24}\text{H}_{12}^{1+}$ | 39.1 | 22.2 | 6.9 | — | — | — | — | — | — | 23.3 | 8.6 | — |
| | $\text{C}_{24}\text{H}_{12}^{2+}$ | 43.5 | — | 26.2 | — | 12.5 | — | — | — | — | 15.2 | — | — |
| | $\text{C}_{24}\text{H}_{12}^{3+}$ | 12.9 | 19.4 | 18.3 | 15.3 | 12.3 | 8.1 | 2.6 | — | — | 6.3 | 4.8 | — |
| 300 keV | $\text{C}_{24}\text{H}_{12}^{1+}$ | 27.6 | 30.6 | 12.5 | 6.7 | — | — | — | — | — | 16.3 | 6.2 | — |
| | $\text{C}_{24}\text{H}_{12}^{2+}$ | 31.4 | — | 35.3 | — | 21.7 | — | 7.7 | — | 3.9 | — | — | — |
| | $\text{C}_{24}\text{H}_{12}^{3+}$ | 10.3 | 14.3 | 18.5 | 16.9 | 14.5 | 10.4 | 3.7 | 2.1 | 5.7 | 2.8 | — | — |

the cation, di-cation and tri-cation spectrum the loss of several (up to eight) hydrogen atoms are clearly observed. The even number of hydrogen losses is more prominent than the odd ones in the doubly charged coronene ions. The loss of the hydrogen in PAHs through ionizing radiation may be a possible source the presence of the H_2 in space and therefore the present study along with the earlier ones may help towards a better understanding of

the H_2 -formation in the ISM.

Acknowledgments

The authors are thankful to the staff of the ECRIA-laboratory of TIFR.

REFERENCES

-
- * ltribedi@gmail.com
- [1] C Joblin, JP Maillard, L d'Hendecourt, and A Leger. Detection of diffuse interstellar bands in the infrared. *Nature*, 346:729–731, 1990.
 - [2] George H Herbig. The diffuse interstellar bands. *Annual Review of Astronomy and Astrophysics*, 33(1):19–73, 1995.
 - [3] Farid Salama, ELO Bakes, LJ Allamandola, and AGGM Tielens. Assessment of the polycyclic aromatic hydrocarbon–diffuse interstellar band proposal. *Astrophysical Journal v. 458*, p. 621, 458:621, 1996.
 - [4] LJ Allamandola, AGGM Tielens, and JRz Barker. Polycyclic aromatic hydrocarbons and the unidentified infrared emission bands–auto exhaust along the milky way. *Astrophysical Journal, Part 2-Letters to the Editor (ISSN 0004-637X)*, vol. 290, March 1, 1985, p. L25-L28., 290:L25–L28, 1985.
 - [5] LJ Allamandola, AGGM Tielens, and JR Barker. Interstellar polycyclic aromatic hydrocarbons–the infrared emission bands, the excitation/emission mechanism, and the astrophysical implications. *Astrophysical Journal Supplement Series (ISSN 0067-0049)*, vol. 71, Dec. 1989, p. 733-775. *Research supported by NASA, DOE, and NSF.*, 71:733–775, 1989.
 - [6] Adolf N Witt, Steve Mandel, Paul H Sell, Thomas Dixon, and Uma P Vijh. Extended red emission in high galactic latitude interstellar clouds. *The Astrophysical Journal*, 679(1):497, 2008.
 - [7] O Berne, C Joblin, M Rapacioli, J Thomas, J-C Cuillandre, and Y Deville. Extended red emission and the evolution of carbonaceous nanograins in ngc 7023. *Astronomy & Astrophysics*, 479(3):L41–L44, 2008.
 - [8] Young Min Rhee, Timothy J Lee, Murthy S Gudipati, Louis J Allamandola, and Martin Head-Gordon. Charged polycyclic aromatic hydrocarbon clusters and the galactic extended red emission. *Proceedings of the National Academy of Sciences*, 104(13):5274–5278, 2007.
 - [9] G Moreels, J Clairemidi, P Hermine, P Brechignac, and P Rousselot. Detection of a polycyclic aromatic molecule in comet phalley. *Astronomy & Astrophysics (ISSN 0004-6361)*, vol. 282, no. 2, p. 643-656, 282:643–656, 1994.
 - [10] LJ Allamandola, DM Hudgins, and SA Sandford. Modeling the unidentified infrared emission with combinations of polycyclic aromatic hydrocarbons. *The Astrophysical Journal*, 511(2):L115, 1999.
 - [11] Anne IS Holm, Henrik AB Johansson, Henrik Cederquist, and Henning Zettergren. Dissociation and multiple ionization energies for five polycyclic aromatic hydrocarbon molecules. *The Journal of chemical physics*, 134(4), 2011.
 - [12] AGGM Tielens. The molecular universe. *Reviews of Modern Physics*, 85(3):1021, 2013.
 - [13] Anne IS Holm, Henning Zettergren, Henrik AB Johansson, Fabian Seitz, Stefan Rosen, Henning T Schmidt, A Lawicki, Jimmy Rangama, Patrick Rousseau, Michael Capron, et al. Ions colliding with cold polycyclic aromatic hydrocarbon clusters. *Physical review letters*, 105(21):213401, 2010.
 - [14] A Leger and JLz Puget. Identification of the unidentified ir emission features of interstellar dust? *Astronomy and Astrophysics (ISSN 0004-6361)*, vol. 137, no. 1, Aug. 1984, p. L5-L8., 137:L5–L8, 1984.
 - [15] A. Lawicki, A. I. S. Holm, P. Rousseau, M. Capron, R. Maisonnay, S. Maclot, F. Seitz, H. A. B. Johansson, S. Rosen, H. T. Schmidt, H. Zettergren, B. Manil, L. Adoui, H. Cederquist, and B. A. Huber. Multiple ionization and fragmentation of isolated pyrene and coronene molecules in collision with ions. *Phys. Rev. A*, 83:022704, Feb 2011.
 - [16] Chandan Bagdia, Shubhadeep Biswas, Anuvab Mandal, Shamik Bhattacharjee, and Lokesh C Tribedi. Ionization and fragmentation of fluorene upon 250 kev proton impact. *The European Physical Journal D*, 75:1–7, 2021.
 - [17] Tao Chen, Michael Gatchell, Mark H Stockett, R Delaunay, Alicja Domaracka, Elisabetta R Micelotta, Alexander GGM Tielens, Patrick Rousseau, Lamri Adoui, Bernd A Huber, et al. Formation of h2 from internally heated polycyclic aromatic hydrocarbons: Excitation energy dependence. *The Journal of chemical physics*, 142(14):144305, 2015.
 - [18] Tao Chen, Michael Gatchell, Mark H Stockett, John D Alexander, Y Zhang, Patrick Rousseau, A Domaracka, S Maclot, R Delaunay, L Adoui, et al. Absolute fragmentation cross sections in atom-molecule collisions: Scaling laws for non-statistical fragmentation of polycyclic aromatic hydrocarbon molecules. *The Journal of chemical physics*, 140(22), 2014.
 - [19] G Vidali, D Jing, and J He. Hydrogen and water in the interstellar medium. In *AIP Conference Proceedings*, volume 1543, pages 31–47. American Institute of Physics, 2013.
 - [20] Robert J Gould and Edwin E Salpeter. The interstellar abundance of the hydrogen molecule. i. basic processes. *Astrophysical Journal*, vol. 138, p. 393, 138:393, 1963.
 - [21] Valentine Wakelam, Emeric Bron, Stephanie Cazaux, Francois Dulieu, Cecile Gry, Pierre Guillard, Emilie Habart, Liv Hornekaer, Sabine Morisset, Gunnar Nyman, et al. H2 formation on interstellar dust grains: The viewpoints of theory, experiments, models and observations. *Molecular Astrophysics*, 9:1–36, 2017.
 - [22] L Boschman. Hydrogenation of pah cations boschman, l.; reitsma, g.; cazaux, s.; schlatholter, thomas; hoekstra, r.; spaans, m.; gonzalez magana, olmo. *THE ASTROPHYSICAL JOURNAL LETTERS*, 761(L33):5pp, 2012.
 - [23] Benedikte Klaerke, Y Toker, Dennis Bo Rahbek, Liv Hornekaer, and Lars Henrik Andersen. Formation and stability of hydrogenated pahs in the gas phase. *Astronomy and Astrophysics*, 549:A84, 2013.
 - [24] Ricardo M Ferullo, Carolina E Zubieta, and Patricia G Belevi. Hydrogenated polycyclic aromatic hydrocarbons (h n pahs) as catalysts for hydrogenation reactions in the interstellar medium: a quantum chemical model. *Physical Chemistry Chemical Physics*, 21(22):12012–12020, 2019.
 - [25] J-P Champeaux, Patrick Moretto-Capelle, Pierre Caffarelli, Charlotte Deville, Martine Sence, and Romain Casta. Is the dissociation of coronene in stellar winds a source of molecular hydrogen? application to the hd 44179 nebula. *Monthly Notices of the Royal Astronomical Society*, 441(2):1479–1487, 2014.
 - [26] M Giard, JP Bernard, A Klotz, I Ristorcelli, C Pech, P Boissel, M Armengaud, P Frabel, and C Joblin. Pho-

- tophysics of interstellar pahas in the pirenea experiment. *European Astronomical Society Publications Series*, 4:297–297, 2002.
- [27] C Joblin, L d’Hendecourt, A Leger, and D Defourneau. Infrared spectroscopy of gas-phase pah molecules. 1: Role of the physical environment. *Astronomy and Astrophysics (ISSN 0004-6361)*, vol. 281, no. 3, p. 923–936, 281:923–936, 1994.
- [28] AN Agnihotri, AH Kelkar, S Kasthurirangan, KV Thulasiram, CA Desai, WA Fernandez, and LC Tribedi. An ecr ion source based low energy ion accelerator: development and performance. *Physica Scripta*, 2011(T144):014038, 2011.
- [29] Anuvab Mandal and LC Tribedi. Gas mixing effect on kr ion currents from an ecr ion source. *Nuclear Instruments and Methods in Physics Research Section B: Beam Interactions with Materials and Atoms*, 440:19–24, 2019.
- [30] Shubhadeep Biswas and Lokesh C Tribedi. A recoil ion momentum spectrometer for probing ionization, e-capture, and capture-ionization induced molecular fragmentation dynamics. *Review of Scientific Instruments*, 92(12), 2021.
- [31] Yu A Dyakov, C-K Ni, SH Lin, YT Lee, and AM Mebel. Ab initio and rrkm study of photodissociation of azulene cation. *Physical Chemistry Chemical Physics*, 8(12):1404–1415, 2006.
- [32] M Krems, J Zirbel, M Thomason, and Robert D DuBois. Channel electron multiplier and channelplate efficiencies for detecting positive ions. *Review of Scientific Instruments*, 76(9), 2005.
- [33] Steven T Manson and JH McGuire. Ratio of double to single ionization of helium: The relationship between ionization by photons and by bare charged particles. *Physical Review A*, 51(1):400, 1995.
- [34] Jim H McGuire, Nora Berrah, Roger J Bartlett, James AR Samson, John A Tanis, C Lewis Cocke, and Alfred S Schlachter. The ratio of cross sections for double to single ionization of helium by high energy photons and charged particles. *Journal of Physics B: Atomic, Molecular and Optical Physics*, 28(6):913, 1995.
- [35] RD DuBois and LH Toburen. Single and double ionization of helium by neutral-particle to fully stripped ion impact. *Physical Review A*, 38(8):3960, 1988.
- [36] WR Thompson, MB Shah, and HB Gilbody. Single and double ionization of atomic oxygen by electron impact. *Journal of Physics B: Atomic, Molecular and Optical Physics*, 28(7):1321, 1995.
- [37] Antonio CF Santos, Ahmad Hasan, and Robert D DuBois. Doubly differential cross sections for single and multiple ionization of ne by electron impact. *Physical Review A*, 71(3):034701, 2005.
- [38] Jim H McGuire, Nora Berrah, Roger J Bartlett, James AR Samson, John A Tanis, C Lewis Cocke, and Alfred S Schlachter. The ratio of cross sections for double to single ionization of helium by high energy photons and charged particles. *Journal of Physics B: Atomic, Molecular and Optical Physics*, 28(6):913, 1995.
- [39] John F Reading, AL Ford, and Xushan Fang. Projectile angular dependence of the ratio of double to single ionization produced by fast protons in collision with helium. *Physical review letters*, 62(3):245, 1989.
- [40] James AR Samson. Proportionality of electron-impact ionization to double photoionization. *Physical review letters*, 65(23):2861, 1990.
- [41] Shubhadeep Biswas and LC Tribedi. Plasmon-mediated electron emission from the coronene molecule under fast ion impact. *Physical Review A*, 92(6):060701, 2015.
- [42] Shubhadeep Biswas, Christophe Champion, PF Weck, and Lokesh C Tribedi. Differential electron emission from polycyclic aromatic hydrocarbon molecules under fast ion impact. *Scientific reports*, 7(1):5560, 2017.
- [43] Junfeng Zhen, Pablo Castellanos, Daniel M Paardeckooper, Niels Ligterink, Harold Linnartz, Laurent Nahon, Christine Joblin, and Alexander GGM Tielens. Laboratory photo-chemistry of pahas: ionization versus fragmentation. *The Astrophysical Journal Letters*, 804(1):L7, 2015.
- [44] Junfeng Zhen, Sarah Rodriguez Castillo, Christine Joblin, Giacomo Mulas, Hassan Sabbah, Alexandre Giuliani, Laurent Nahon, Serge Martin, Jean-Philippe Champeaux, and Paul M Mayer. Vuv photo-processing of pah cations: quantitative study on the ionization versus fragmentation processes. *The Astrophysical Journal*, 822(2):113, 2016.
- [45] Christine Joblin, Gabi Wenzel, S Rodriguez Castillo, Aude Simon, Hassan Sabbah, Anthony Bonnamy, Dominique Toubanc, Giacomo Mulas, Mingchao Ji, Alexandre Giuliani, et al. Photo-processing of astro-pahas. In *Journal of Physics: Conference Series*, volume 1412, page 062002. IOP Publishing, 2020.